Chapter 5

Interaction between interfacial collinear Griffith cracks in composite media under thermal loading

5.1 Introduction

It looks that microscopic flows do not lead to safe structure to fail. Sometimes it becomes very expensive to replace the component of engineering structures. In fact, on one hand, due to increasing demands for energy and material conservations, the safety margins assigned to structures have to be smaller. On the other hand, the detection of a flaw in a structure does not automatically mean that it is not safe to use anymore. This is particularly relevant in the case of expensive materials or components of structures whose usage it would be inconvenient to interrupt. In this setting fracture mechanics plays a key role during the analysis of materials which exhibits cracks and also to predict whether and in which manner failure may occurs.

A property of a structure relating to its ability to sustain defects until repair is called damage tolerance. During design of engineering structures the damage tolerance is always taken in account as it is assumed that flaws can exist in any structure and such flaws propagate with usage. In aerospace engineering structures this approach is necessary to avoid the extension of cracks. In fracture mechanics crack growth is exponential in nature i.e., the crack growth rate is a function of an exponent of crack size according to the Paris law. The exponential crack growths led to the development of non-destructive testing methods through which the structural engineers may inspect

---

The contents of this chapter have been published in **Zeitschrift fur Naturforschung A / A Journal of Physical Sciences.**

invisible cracks occur in structures which grow slowly. So amounts of maintenance checks are reduced by non destructive inspections. Crack propagation and arrest have become important topics in a structure containing isolated region of an unstable crack growth. So emergence of an unstable crack from bad region can still be arrested using the surrounding of good materials, provided good materials have sufficiently high fracture toughness i.e., materials have large resistance to protect the structure from crack propagation. This clearly exhibits the importance of studying propagation of cracks occur in structures and the arrest of crack propagation for the safety of the structure. The physical quantities like stress intensity factor, crack energy, stress magnification factor play important roles during the study of crack arrest (Melville (1977), Rose (1986), Misra and Sukere (1991), Priest (1998), Bousquet et al. (2012)).

Problems consist of heat and deformation has attracted much interest to the scientists and engineers for last couple of decades. The thermal stress concentration near the crack tips has becomes an interesting topic of research nowadays. In the formation of structural members of airplanes, motor vehicles and high speed trains, composite materials are used widely due to their light weight and strong nature. When a cracked structural member is subject to different temperature fields, then the evaluation of stress intensity factors becomes essential due to disturbance in heat flux. The study of thermal stress around the cracked surface becomes important for the prediction of stability and service life of cracked engineering materials and structures. In linear elastic fracture mechanics the study of geometry of collinear cracks has practical importance as pre-existing cracks lead to fracture due to interaction of cracks which forms a major crack in a medium. Noda and Wang (2002) have studied the interaction between collinear cracks situated in an inhomogeneous medium under transient loading. During thermo elastic analysis of a cracked solid, a considerable effort has been given by the researchers based on the theory of the thermo-elasticity. Sih (1962) observed the singular character of thermal stress near a crack in an infinite plate when heat flows perpendicular to the crack. A solution of a thermo-elastic crack problem had been given by Atkinson and Clement (1977) in an anisotropic medium with single crack. Applying the method given by Muskhelishvili (1953), Clement (1983) solved the thermo-elastic crack problem bonded between dissimilar anisotropic materials. He assumed that the heat flows through the two surfaces of a crack equally but opposite in direction. Clement and Tauchert (1979) have studied thermo-elastic crack problem for an anisotropic slab. Sekine (1977) calculated the thermal stresses near the crack tips of an isolated line crack in a semi infinite medium subjected to uniform heat flow. Same author studied thermo-elastic interaction between two cracks (1979). Itou (1991) has calculated the thermal stresses around an isolated crack in an infinite elastic strip in which the surfaces of the strip are maintained at different temperature. Itou and Rengen (1993) studied the thermal stresses around two parallel cracks situated at the interface positions of two bonded dissimilar elastic half planes. Itou and Rengen (1995) have solved a problem of two collinear cracks in an adhesive layer sandwiched between two dissimilar elastic half planes. In Thermal stresses in an infinite orthotropic plate around two parallel cracks under uniform heat flow were evaluated by Itou (2001). Zhou et al. (2007) have investigated transient two dimensional thermal crack problem in a functionally graded orthotropic strip using Laplace and Fourier transform technique. Baksi et al. (2007) have determined the thermal stresses and displacement fields in an orthotropic plane containing a pair of equal collinear Griffith cracks using integral transform technique based upon displacement potential functions under steady state temperature field. Zhong et al. (2013) have investigated the thermal stress around two collinear Griffith cracks in an orthotropic solid subjected to thermo-mechanical loading using Fourier transform technique. Recently, Itou (2014) has calculated the thermal stress in an infinite orthotropic plane around two upper collinear cracks placed parallel to a lower crack. Problem related to thermal stress can also be found in the research articles of Noda et al. (2003) and Hetnarski and Ignaczak. But to the best of my knowledge the problem related to interaction between interfacial cracks under thermo-mechanical loading are not yet been done by any researcher.

The main goal of this chapter is to analyze the interaction among three collinear Griffith cracks situated at the interface of two orthotropic thermo-elastic half planes under uniform heat flux. To study the effect of temperature on displacements and stresses, an integral technique has been applied. The problem is reduced to a dual form of the integral equations, which is solved numerically using Jacobi polynomials. The expressions of SIFs at the tips of the cracks are found analytically. The graphical presentations of the effect of outer cracks on the propagation of central crack and also the propagation tendency of outer crack due to presence of central one for different particular cases are the key feature of the present chapter.

5.2 Problem formulation

Consider two bonded homogeneous orthotropic elastic half planes $y \geq 0$ and $y \leq 0$ containing three collinear Griffith cracks at the interface $y = 0$ when Cartesian co-ordinate axes coincide with the axes of symmetry of the elastic material. Here the geometry of this chapter is different from the previous one. The temperature distribution functions $T^{(i)}(x, y)$, $(i = 1,\ 2)$ under the steady state condition are assumed to satisfy the heat conduction equation (4.1) in the considered orthotropic media. The resultant temperature distribution under the prescribed heat source $\delta(x)$ is given in equation (4.8).The relations between plane stress induced by the distributions of temperature and displacement components $u^{(i)}(x,y)$ and $v^{(i)}(x,y)$ along x and y directions are given in equations (4.9)-(4.11).

The displacement equations of equilibrium are as given in equations (4.12) and (4.13). It is assumed that at the interface $y=0$, the central crack defined by $|x|<a$ and the outer defined by $b<|x|<1$ are opened by internal normal and shearing tractions $p_1(x)$ and $p_2(x)$ respectively (Fig. 5.1). The boundary conditions on $y=0$ are given by

$$\sigma_{yy}^{(1)}(x,0) = -p_1(x),\ 0\le|x|\le a,\ b\le|x|\le 1, \tag{5.1}$$

$$\sigma_{xy}^{(1)}(x,0) = -p_2(x),\ 0\le|x|\le a,\ b\le|x|\le 1, \tag{5.2}$$

$$u^{(1)}(x,0) = u^{(2)}(x,0),\ a<|x|<b,\ 1<|x|<\infty, \tag{5.3}$$

$$v^{(1)}(x,0) = v^{(2)}(x,0),\ a<|x|<b,\ 1<|x|<\infty, \tag{5.4}$$

$$\sigma_{yy}^{(1)}(x,0) = \sigma_{yy}^{(2)}(x,0),\quad -\infty<x<\infty, \tag{5.5}$$

$$\sigma_{xy}^{(1)}(x,0) = \sigma_{xy}^{(2)}(x,0),\quad -\infty<x<\infty, \tag{5.6}$$

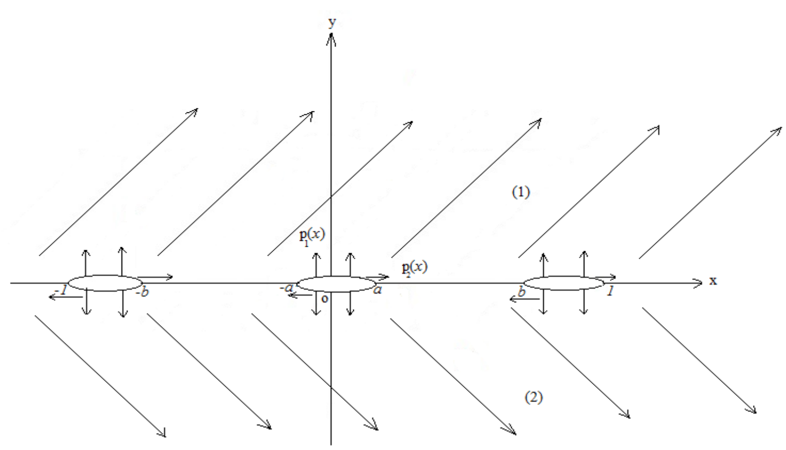

Fig. 5.1 Geometry of the problem

In the Fig. 5.1, the inclined arrows denote the regions for the semi infinite half planes, the vertical arrows denote the direction of the applied normal stress and the horizontal arrows denote the direction of shearing stress for our considered mixed Mode type problem.

5.3 Solution of the problem

During solution of the problem, let us first consider the displacement potentials as given in equation (4.20) and potential functions $\phi_j^{(i)}(x,y)$ for the half planes as given in equations (4.21)-(4.22).

The displacement components $u^{(i)}(x,y)$, $v^{(i)}(x,y)$ and the thermal stresses may be written as equations (4.23) and equations (4.24)-(4.26).

Here potential functions $\phi_j^{(i)}(x,y)$ satisfy the differential equation

$$\left(\frac{\partial^2}{\partial x^2}+\frac{\partial^2}{\partial y^2}\right)\phi_j^{(i)}(x,y)=0,\ i=1,2\ ;\ j=1,2,$$

where $\mu_1^{(i)}$ and $\mu_2^{(i)}$ are the real roots of the equation (4.29) with $k_j^{(i)}$ are given in equation (4.30).

Boundary conditions (5.3) and (5.4) with the help of the boundary conditions (5.5) and (5.6) and the above mentioned equations give rise to

$$\int_0^\infty \left\{\alpha_1+\alpha_2 A_1^{(1)}(s)+\alpha_3 A_2^{(1)}(s)\right\}\frac{\sin(sx)}{s}\,ds=0, \qquad a<x<b,\ 1<x<\infty, \tag{5.7}$$

$$\int_0^\infty \left\{\beta_1+\beta_2 A_1^{(1)}(s)+\beta_3 A_2^{(1)}(s)\right\}\frac{\cos(sx)}{s}\,ds=0, \qquad a<x<b,\ 1<x<\infty, \tag{5.8}$$

where the undetermined functions $A_1^{(i)}(s)$ and $A_2^{(i)}(s)$ $(i=1,2)$ are given by

$$A_1^{(2)}(s)=\frac{k^{(2)}(1+\eta^{(2)})\sqrt{\mu_1^{(2)}}}{2(\sqrt{\mu_2^{(2)}}-\sqrt{\mu_1^{(2)}})(1+k_1^{(2)})}\left(\frac{K^{(2)}-\sqrt{\mu_2^{(2)}}}{K^{(2)}}\right)+\frac{C_{66}^{(1)}}{C_{66}^{(2)}}\frac{k^{(1)}(1+\eta^{(1)})}{2K^{(1)}}\frac{\sqrt{\mu_1^{(2)}}(\sqrt{\mu_{22}^{(2)}}-K^{(1)})}{(1+k_1^{(2)})(\sqrt{\mu_2^{(2)}}-\sqrt{\mu_1^{(2)}})}$$
$$+A_1^{(1)}(s)\frac{\sqrt{\mu_1^{(2)}}(1+k_1^{(1)})(\sqrt{\mu_2^{(2)}}-\sqrt{\mu_1^{(1)}})}{\sqrt{\mu_1^{(1)}}(1+k_1^{(2)})(\sqrt{\mu_2^{(2)}}-\sqrt{\mu_1^{(2)}})}+A_2^{(1)}(s)\frac{\sqrt{\mu_1^{(2)}}(1+k_2^{(1)})(\sqrt{\mu_2^{(2)}}-\sqrt{\mu_2^{(1)}})}{\sqrt{\mu_2^{(1)}}(1+k_1^{(2)})(\sqrt{\mu_2^{(2)}}-\sqrt{\mu_1^{(2)}})},$$

$$A_2^{(2)}(s)=\frac{k^{(2)}(1+\eta^{(2)})\sqrt{\mu_2^{(2)}}}{2(\sqrt{\mu_1^{(2)}}-\sqrt{\mu_2^{(2)}})(1+k_2^{(2)})}\left(\frac{K^{(2)}-\sqrt{\mu_1^{(2)}}}{K^{(2)}}\right)+\frac{C_{66}^{(1)}}{C_{66}^{(2)}}\frac{k^{(1)}(1+\eta^{(1)})}{2K^{(1)}}\frac{\sqrt{\mu_2^{(2)}}(\sqrt{\mu_{21}^{(2)}}-K^{(1)})}{(1+k_2^{(2)})(\sqrt{\mu_1^{(2)}}-\sqrt{\mu_2^{(2)}})}$$

$$+A_1^{(1)}(s)\frac{\sqrt{\mu_2^{(2)}}(1+k_1^{(1)})(\sqrt{\mu_1^{(2)}}-\sqrt{\mu_1^{(1)}})}{\sqrt{\mu_1^{(1)}}(1+k_2^{(2)})(\sqrt{\mu_1^{(2)}}-\sqrt{\mu_2^{(2)}})}+A_2^{(1)}(s)\frac{\sqrt{\mu_2^{(2)}}(1+k_2^{(1)})(\sqrt{\mu_1^{(2)}}-\sqrt{\mu_2^{(1)}})}{\sqrt{\mu_2^{(1)}}(1+k_2^{(2)})(\sqrt{\mu_1^{(2)}}-\sqrt{\mu_2^{(2)}})}.$$

Now setting

$$\alpha_1+\alpha_2A_1^{(1)}(s)+\alpha_3A_2^{(1)}(s)=\int_0^a f_1(t)\cos(st)\,dt+\int_b^1 f_1(t)\cos(st)\,dt,$$

$$\beta_1+\beta_2A_1^{(1)}(s)+\beta_3A_2^{(1)}(s)=\int_0^a f_2(t)\sin(st)\,dt+\int_b^1 f_2(t)\sin(st)\,dt,$$

where

$$\alpha_1=\left(\frac{k^{(1)}-k^{(2)}}{2}\right)-\left(\frac{k^{(2)}(1+\eta^{(2)})\sqrt{\mu_1^{(2)}}}{2(\sqrt{\mu_2^{(2)}}-\sqrt{\mu_1^{(2)}})(1+k_1^{(2)})}\left(\frac{K^{(2)}-\sqrt{\mu_2^{(2)}}}{K^{(2)}}\right)+\frac{C_{66}^{(1)}}{C_{66}^{(2)}}\frac{k^{(1)}(1+\eta^{(1)})}{2K^{(1)}}\frac{\sqrt{\mu_1^{(2)}}(\sqrt{\mu_{22}^{(2)}}-K^{(1)})}{(1+k_1^{(2)})(\sqrt{\mu_2^{(2)}}-\sqrt{\mu_1^{(2)}})}\right)$$

$$-\left(\frac{k^{(2)}(1+\eta^{(2)})\sqrt{\mu_2^{(2)}}}{2(\sqrt{\mu_1^{(2)}}-\sqrt{\mu_2^{(2)}})(1+k_2^{(2)})}\left(\frac{K^{(2)}-\sqrt{\mu_1^{(2)}}}{K^{(2)}}\right)+\frac{C_{66}^{(1)}}{C_{66}^{(2)}}\frac{k^{(1)}(1+\eta^{(1)})}{2K^{(1)}}\frac{\sqrt{\mu_2^{(2)}}(\sqrt{\mu_{21}^{(2)}}-K^{(1)})}{(1+k_2^{(2)})(\sqrt{\mu_1^{(2)}}-\sqrt{\mu_2^{(2)}})}\right),$$

$$\alpha_2=\left(1-\frac{\sqrt{\mu_1^{(2)}}(1+k_1^{(1)})(\sqrt{\mu_2^{(2)}}-\sqrt{\mu_1^{(1)}})}{\sqrt{\mu_1^{(1)}}(1+k_1^{(2)})(\sqrt{\mu_2^{(2)}}-\sqrt{\mu_1^{(2)}})}-\frac{\sqrt{\mu_2^{(2)}}(1+k_1^{(1)})(\sqrt{\mu_1^{(2)}}-\sqrt{\mu_1^{(1)}})}{\sqrt{\mu_1^{(1)}}(1+k_2^{(2)})(\sqrt{\mu_1^{(2)}}-\sqrt{\mu_2^{(2)}})}\right),$$

$$\alpha_3=\left(1-\frac{\sqrt{\mu_1^{(2)}}(1+k_2^{(1)})(\sqrt{\mu_2^{(2)}}-\sqrt{\mu_2^{(1)}})}{\sqrt{\mu_2^{(1)}}(1+k_1^{(2)})(\sqrt{\mu_2^{(2)}}-\sqrt{\mu_1^{(2)}})}-\frac{\sqrt{\mu_2^{(2)}}(1+k_2^{(1)})(\sqrt{\mu_1^{(2)}}-\sqrt{\mu_2^{(1)}})}{\sqrt{\mu_2^{(1)}}(1+k_2^{(2)})(\sqrt{\mu_1^{(2)}}-\sqrt{\mu_2^{(2)}})}\right),$$

$$\beta_1=\left(1-\frac{k^{(1)}\eta^{(1)}}{2K^{(1)}}-\frac{k^{(2)}\eta^{(2)}}{2K^{(2)}}\right),$$

$$\beta_2=\left(\frac{k_1^{(1)}}{\sqrt{\mu_1^{(1)}}}+\frac{k_1^{(2)}}{\sqrt{\mu_1^{(2)}}}\frac{\sqrt{\mu_1^{(2)}}(1+k_1^{(1)})(\sqrt{\mu_2^{(2)}}-\sqrt{\mu_1^{(1)}})}{\sqrt{\mu_1^{(1)}}(1+k_1^{(2)})(\sqrt{\mu_2^{(2)}}-\sqrt{\mu_1^{(2)}})}+\frac{k_2^{(2)}}{\sqrt{\mu_2^{(2)}}}\frac{\sqrt{\mu_2^{(2)}}(1+k_1^{(1)})(\sqrt{\mu_1^{(2)}}-\sqrt{\mu_1^{(1)}})}{\sqrt{\mu_1^{(1)}}(1+k_2^{(2)})(\sqrt{\mu_1^{(2)}}-\sqrt{\mu_2^{(2)}})}\right),$$

$$\beta_3=\left(\frac{k_2^{(1)}}{\sqrt{\mu_2^{(1)}}}+\frac{k_1^{(2)}}{\sqrt{\mu_1^{(2)}}}\frac{\sqrt{\mu_1^{(2)}}(1+k_2^{(1)})(\sqrt{\mu_2^{(2)}}-\sqrt{\mu_2^{(1)}})}{\sqrt{\mu_2^{(1)}}(1+k_1^{(2)})(\sqrt{\mu_2^{(2)}}-\sqrt{\mu_1^{(2)}})}+\frac{k_2^{(2)}}{\sqrt{\mu_2^{(2)}}}\frac{\sqrt{\mu_2^{(2)}}(1+k_2^{(1)})(\sqrt{\mu_1^{(2)}}-\sqrt{\mu_2^{(1)}})}{\sqrt{\mu_2^{(1)}}(1+k_2^{(2)})(\sqrt{\mu_1^{(2)}}-\sqrt{\mu_2^{(2)}})}\right)$$

and after lengthy process of mathematical manipulations, boundary conditions (5.1) and (5.2) finally lead to the following singular integral equations

$$a_1 f_1(x) + \frac{1}{\pi b_1}\int_{-a}^{a}\frac{f_2(t)}{(t-x)}dt + \frac{2}{\pi b_1}\int_{b}^{1}\frac{f_2(t)}{(t-x)}dt = -\frac{2}{\pi}p_1(x), \tag{5.9}$$

$$c_1 f_2(x) + \frac{1}{\pi d_1}\int_{-a}^{a}\frac{f_1(t)}{(t-x)}dt + \frac{2}{\pi d_1}\int_{b}^{1}\frac{f_1(t)}{(t-x)}dt = -\frac{2}{\pi}p_2(x) - \frac{2c}{\pi x}, \tag{5.10}$$

where

$$a_1 = \frac{2}{\pi}C_{66}^{(1)}\left[(1+k_1^{(1)})\left(\frac{\beta_3\beta_1-\alpha_1\alpha_3}{\beta_3\alpha_2-\alpha_3\beta_2}\right)-(1+k_2^{(1)})\left(\frac{\beta_3\beta_1-\alpha_1\alpha_3}{\beta_2\alpha_3-\alpha_2\beta_3}\right)\right],$$

$$\frac{1}{b_1} = \frac{2}{\pi}C_{66}^{(1)}\left[(1+k_1^{(1)})\left(\frac{\alpha_2\alpha_1-\beta_2\beta_1}{\beta_3\alpha_2-\alpha_3\beta_2}\right)-(1+k_2^{(1)})\left(\frac{\alpha_2\alpha_1-\beta_2\beta_1}{\beta_2\alpha_3-\alpha_2\beta_3}\right)\right],$$

$$c_1 = \frac{2}{\pi}C_{66}^{(1)}\left[\frac{(1+k_1^{(1)})}{\sqrt{\mu_1^{(1)}}}\left(\frac{\alpha_2\beta_1-\beta_2\alpha_1}{\beta_3\alpha_2-\alpha_3\beta_2}\right)-\frac{(1+k_2^{(1)})}{\sqrt{\mu_2^{(1)}}}\left(\frac{\alpha_2\beta_1-\beta_2\alpha_1}{\beta_2\alpha_3-\alpha_2\beta_3}\right)\right],$$

$$\frac{1}{d_1} = \frac{2}{\pi}C_{66}^{(1)}\left[\frac{(1+k_1^{(1)})}{\sqrt{\mu_1^{(1)}}}\left(\frac{\beta_3\alpha_1-\beta_1\alpha_3}{\beta_3\alpha_2-\alpha_3\beta_2}\right)-\frac{(1+k_2^{(1)})}{\sqrt{\mu_2^{(1)}}}\left(\frac{\beta_3\alpha_1-\beta_1\alpha_3}{\beta_2\alpha_3-\alpha_2\beta_3}\right)\right],$$

$$c = \frac{2}{\pi}C_{66}^{(1)}\left[\frac{(1+k_1^{(1)})}{\sqrt{\mu_1^{(1)}}}\left(\frac{\alpha_3\beta_1-\alpha_1\beta_3}{\beta_3\alpha_2-\alpha_3\beta_2}\right)+\frac{(1+k_2^{(1)})}{\sqrt{\mu_2^{(1)}}}\left(\frac{\alpha_2\beta_1-\alpha_1\beta_2}{\beta_2\alpha_3-\alpha_2\beta_3}\right)+\frac{(1+\eta^{(1)})}{2}\frac{k^{(1)}}{K^{(1)}}\right].$$

Equations (5.9) and (5.10) are reduced to the following singular integral equations for the determination of unknown functions $f_i(x)$

$$\phi_k(x) + \frac{1}{\pi\, i\,\varepsilon\, r_k}\int_{-a}^{a}\frac{\phi_k(t)}{(t-x)}dt + \frac{2}{\pi\, i\,\varepsilon\, r_k}\int_{b}^{1}\frac{\phi_k(t)}{(t-x)}dt = -g_k(x) - \frac{2ic}{\pi r_k x}, \tag{5.11}$$

where $f_i(x)$ satisfy the conditions

$$\int_{-a}^{a} f_i(t)\,dt = 0 \;\text{ and }\; \int_{b}^{1} f_i(t)\,dt = 0, \quad i = 1,2, \tag{5.12}$$

where $\phi_k(x) = \sqrt{a_1 b_1}\, f_1(x) + i r_k\sqrt{c_1 d_1}\, f_2(x), \quad k = 1, 2,$

$\varepsilon = \sqrt{a_1 b_1 c_1 d_1}$, $r_k = (-1)^{k+1}$, $k = 1, 2,$

$$g_k(x) = \frac{2}{\pi}[\sqrt{b_1 / a_1}\, p_1(x) + r_k \sqrt{d_1 / c_1}\, p_2(x)], \qquad k = 1, 2.$$

The solution of above integral equations (5.11) may be assumed as

$$\phi_k(x) = \omega_k(x) \sum_{n=0}^{\infty} c_{kn} P_n^{(\alpha_k, \beta_k)}(x), \qquad k = 1, 2, \tag{5.13}$$

where $\omega_k(x) = (1-x)^{\alpha_k}(1+x)^{\beta_k}$,

$\alpha_k = -\frac{1}{2} + i\omega_k$, $\beta_k = -\frac{1}{2} - i\omega_k$, $\omega_k = r_k \omega$,

and $\omega = \frac{1}{2\pi} \ln\left|\frac{1+\varepsilon}{1-\varepsilon}\right|$,

with c_{kn} are unknown constants. Now using equation (5.12), we get

$\int_{-1}^{1} \phi_i(t)dt = 0$, and $\int_{b/a}^{1/a} \phi_i(t)dt = 0$, $i = 1, 2,$

which implies $c_{k0} = 0$, $k = 1, 2.$

From equations (5.11) and (5.13), we get

$$\frac{\sqrt{1-\varepsilon^2}}{2 i \varepsilon r_k} \sum_{n=1}^{\infty} c_{kn} P_{n-1}^{(-\alpha_k, -\beta_k)}(x) + \frac{2}{\pi i \varepsilon r_k} \int_{b/a}^{1/a} \frac{\omega_k(t) \sum_{n=0}^{\infty} c_{kn} P_n^{(\alpha_k, \beta_k)}(t)}{(t-x)} dt = -g_k(x) - \frac{2 i c}{\pi r_k} \sqrt{\frac{d_1}{c_1}} \frac{1}{x}. \tag{5.14}$$

Multiplying the above equation by $\omega_k^{-1}(x) P_j^{(-\alpha_k, -\beta_k)}(x)$ and integrating from -1 to 1with respect to x, we get

$$c_{k\, j+1} \theta_j^{(\alpha_k, \beta_k)} + \frac{2}{\pi i \varepsilon_k r_k} \sum_{n=1}^{\infty} c_{kn} L_{njk} = -F_{kj} - \frac{2 i c}{\pi r_k} \sqrt{\frac{d_1}{c_1}} \int_{-1}^{1} \frac{\omega_k^{-1}(x) P_j^{(\alpha_k, \beta_k)}(x)}{x} dx, \tag{5.15}$$

where $\theta_j^{(\alpha_k, \beta_k)} = \frac{\sqrt{1-\varepsilon^2}}{i \varepsilon r_k} \left(\frac{\Gamma(j - \alpha_k + 1)\Gamma(j - \beta_k + 1)}{\Gamma(j+2)\ j+1!} \right)$,

$L_{njk} = \int_{-1}^{1} \omega_k^{-1}(x) P_j^{(-\alpha_k, -\beta_k)}(x) \int_{b/a}^{1/a} \frac{\omega_k(t) P_n^{(\alpha_k, \beta_k)}(t)}{(t-x)} dt\, dx$, $F_{kj} = \int_{-1}^{1} \omega_k^{-1}(x) g_k(x) P_j^{(-\alpha_k, -\beta_k)}(x)\, dx$, with $k=1,2$, $j=0,1$.

Finally the stress intensity factors at the crack tips at $x=a$, $x=b$ and $x=1$ are calculated as

$$\sqrt{b_1/a_1}\ K_I{}^a + ir_k\sqrt{d_1/c_1}\ K_{II}{}^a = \lim_{x\to a+}(x-a)^{-\alpha_k}(x+a)^{-\beta_k}[\sqrt{b_1/a_1}\sigma_{yy}^{(1)}(x,0)+ir_k\sqrt{d_1/c_1}\sigma_{xy}^{(1)}(x,0)]$$

$$=\frac{(-1)^{\alpha_k}\pi a}{2}\sum_{n=1}^{\infty}c_{kn}P_n^{(\alpha_k,\beta_k)}(1),\quad k=1,2. \tag{5.16}$$

$$\sqrt{b_1/a_1}\ K_I{}^b + ir_k\sqrt{d_1/c_1}\ K_{II}{}^b = \lim_{x\to b-}(x-b)^{-\alpha_k}(x+b)^{-\beta_k}[\sqrt{b_1/a_1}\sigma_{yy}^{(1)}(x,0)+ir_k\sqrt{d_1/c_1}\sigma_{xy}^{(1)}(x,0)]$$

$$=\frac{(-1)^{\alpha_k}\pi b}{2}\sum_{n=1}^{\infty}c_{kn}P_n^{(\alpha_k,\beta_k)}(1),\quad k=1,2. \tag{5.17}$$

$$\sqrt{b_1/a_1}\ K_I{}^1 + ir_k\sqrt{d_1/c_1}\ K_{II}{}^1 = \lim_{x\to 1+}(x-1)^{-\alpha_k}(x+1)^{-\beta_k}[\sqrt{b_1/a_1}\sigma_{yy}^{(1)}(x,0)+ir_k\sqrt{d_1/c_1}\sigma_{xy}^{(1)}(x,0)]$$

$$=\frac{(-1)^{\alpha_k}\pi}{2}\sum_{n=1}^{\infty}c_{kn}P_n^{(\alpha_k,\beta_k)}(1),\qquad k=1,2. \tag{5.18}$$

Now stress magnification factors (SMF) are defined by $M_I^a=\dfrac{K_I^a}{K_I^{a^*}}$, $M_I^b=\dfrac{K_I^b}{K_I^{b^*}}$, $M_I^1=\dfrac{K_I^1}{K_I^{1^*}}$ and $M_{II}^a=\dfrac{K_{II}^a}{K_{II}^{a^*}}$, $M_{II}^b=\dfrac{K_{II}^b}{K_{II}^{b^*}}$, $M_{II}^1=\dfrac{K_{II}^1}{K_{II}^{1^*}}$, where $K_I^{a^*}$ and $K_{II}^{a^*}$ are the Mode-I and Mode-II stress intensity factors at $x=a$ due to presence of only central crack situated at the interface of two half planes. $K_I^{b^*}$, $K_{II}^{b^*}$ and $K_I^{1^*}$, $K_{II}^{1^*}$ are the stress intensity factors at $x=b$ and $x=1$ respectively due to presence of only outer cracks situated at the interface of two half planes.

5.4 Results and discussion

In this section, the numerical computations have been done to find stress intensity factors and stress magnification factors for three collinear cracks situated at the interface of two orthotropic materials as α-Uranium and Epoxy Boron, whose elastic constants are already given in section 4.4 in the chapter 4.

During computations the loadings are considered to be $p_1(x) = p$, $p_2(x) = 0$. The dimensionless stress magnification factors for both the types Mode-I and Mode-II at the tip of the central crack $x = a$ are described through Fig. 5.2 and Fig. 5.3 respectively for different values of dimensionless quantity b/a keeping $a = 0.5$ and varying $b = 0.6\ (0.1)\ 0.9$. Again keeping the outer crack length fixed $b = 0.6$ and varying $a = 0.1\ (0.1)\ 0.5$, the stress magnification factors at the outer crack tips $x = b$ and $x = 1$ are depicted through Figs. 5.4 - 5.5 and Figs. 5.6 - 5.7 respectively for various values of b/a for Mode-I and Mode-II types.

It is seen from Fig. 5.2 that as the length of the outer crack increases, then stress magnification factor M_I^a decreases. This is due to the formation of large plastic zone with the increase of crack length at the vicinity of the crack tip which resists the propagation of the crack. To overcome the effect of the plasticity, we have either to increase the crack length or have to apply more thermo- mechanical load. If we further increase the crack length then stress magnification factor oscillates which shows the plastic behavior i.e., crack reaches in plastic region causes crack propagation tendency. Same type of behavior is observed through Fig. 5.4 for stress magnification factor M_I^b.

It is seen from the Fig. 5.3 and Fig. 5.5 that there is a possibility of shielding with increase in crack length whereas Fig. 5.6 and Fig. 5.7 show that there is a possibility of amplification. Thus the propagation tendency at $x = 1$ of outer interfacial crack increases with increase of central crack length.

The variations of Mode-II stress magnification factor depend upon the crack separation distance and crack length. Fig. 5.3 shows that central crack experiences shielding effect due to the presence of outer crack. This effect is maximum when outer crack size is minimum and crack separation distance between the outer crack and central crack is maximum. As the length of the outer crack decreases together with simultaneous increase in crack separation, the shielding effect increases gradually. When the outer crack size is 40% and crack separation distance is 10% of main crack size then shielding is about 45%. When the size of the outer cracks are one- twentieth and crack separation is nine –twentieth to the central crack then shielding is about 80%.

Fig. 5.5 reveals that outer crack experiences shielding effect due to the presence of central crack. This effect is maximum when central crack size is maximum and crack separation distance between the outer crack and central crack is minimum. As the length of the central crack decreases together with simultaneous increase in crack separation distance, the shielding effect gradually decreases. When the central crack size is 120% and crack separation distance is 25% to the outer crack size then shielding is about 80%. When the size of the central crack is half and crack separation is five-forth to the outer crack then shielding is about 60%.

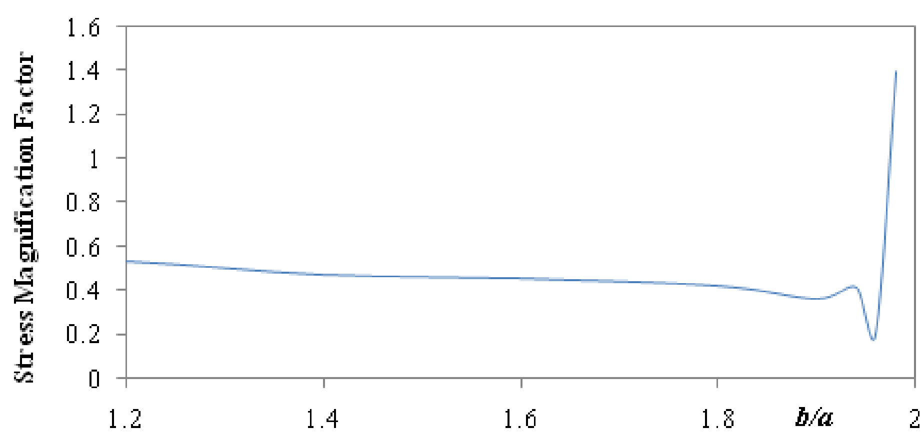

Fig. 5.2 Plot of M_I^a vs. *b/a* at *a=0.5*

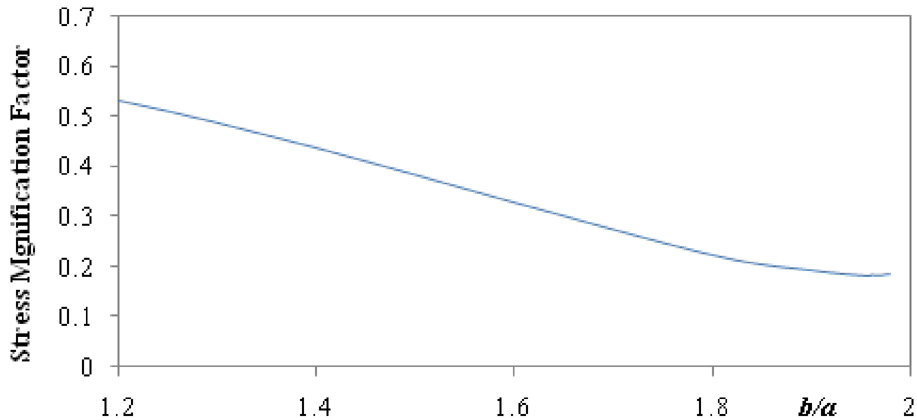

Fig. 5.3 Plot of M_{II}^{a} vs. *b/a* at *a=0.5*

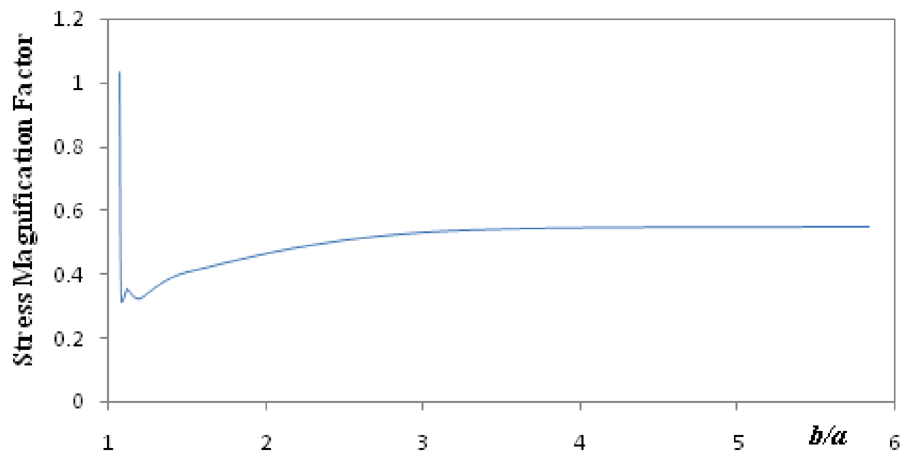

Fig. 5.4 Plot of M_{I}^{b} vs. *b/a* at *b=0.6*

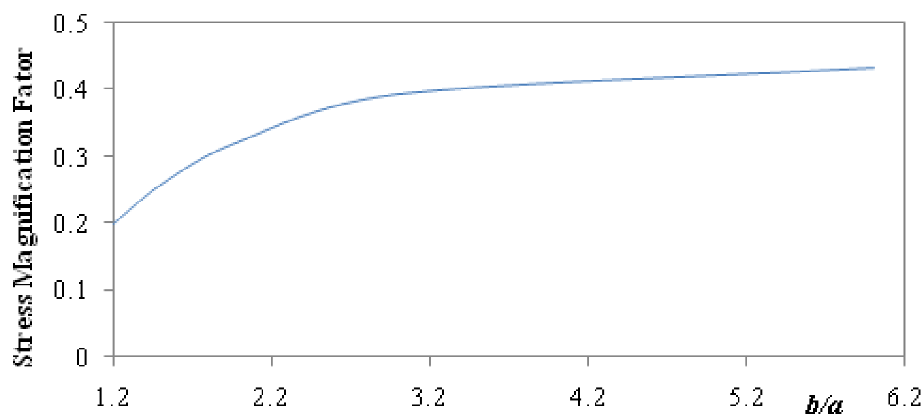

Fig. 5.5 Plot of M_{II}^{b} vs. *b/a* at *b=0.6*

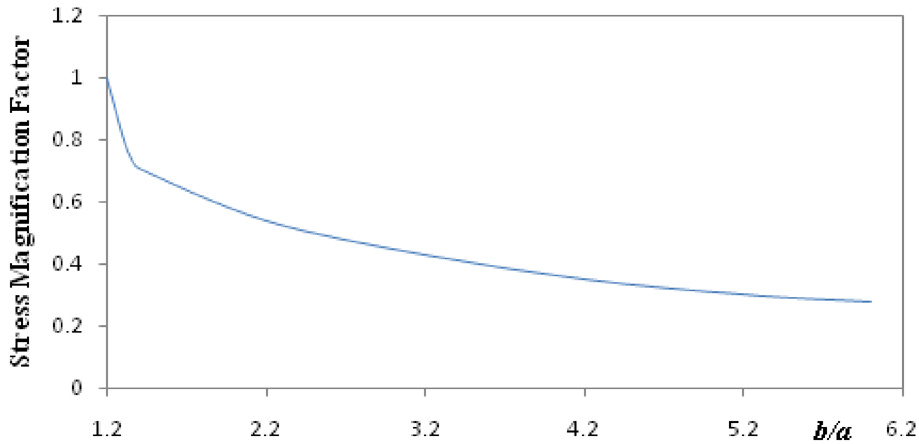

Fig. 5.6 Plot of M_I^1 vs. *b/a* at *b=0.6*

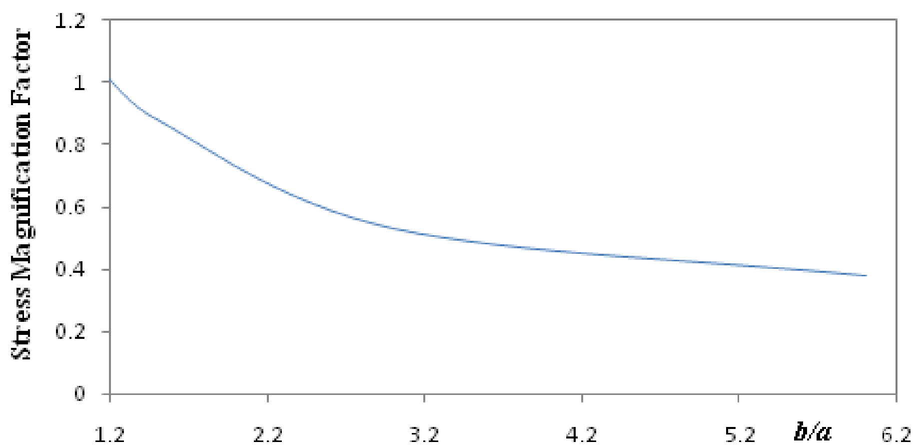

Fig. 5.7 Plot of M_{II}^1 vs. *b/a* at *b=0.6*

5.5 Conclusion

In the present chapter three important goals have been achieved. The first one is the investigation of three collinear cracks at the interface of two orthotropic media under thermo- mechanical loading. Second one is finding the analytical form of the stress intensity factors at the vicinity of the crack tips. Third one is the graphical presentations of amplification and shielding effect through the stress magnification factors which help to find the possibilities of arrest of central crack due to the presence of outer cracks and vice-versa.